Received ; | Revised ; | Accepted

DOI: xxx/xxxx

ARTICLE TYPE

Phase transition in a stochastic geometry model with applications to statistical mechanics

O. K. Kazemi[1] | A. Pourdarvish*[1] | J. Sadeghi[2]

[1] Institute of Mathematics, Department of Statistics, University of Mazandaran, Babolsar, Iran

[2]Department of Physic, University of Mazandaran, Babolsar, Iran

Correspondence

*Ahmad Pourdarvish, Institute of Mathematics, University of Mazandaran, Babolsar, Iran. Email: a.pourdarvish@umz.ac.ir

Summary

We study the connected components of the stochastic geometry model on Poisson points which is obtained by connecting points with a probability that depends on their relative position. Equivalently, we investigate the random clusters of the random connection model defined on the points of a Poisson process in d-dimensional space where the links are added with a particular probability function. We use the thermodynamic relations between free energy, entropy and internal energy to find the functions of the cluster size distribution in the statistical mechanics of extensive and non-extensive. By comparing these obtained functions with the probability function predicted by Penrose, we provide a suitable approximate probability function. Moreover, we relate this stochastic geometry model to the physics literature by showing how the fluctuations of the thermodynamic quantities of this model correspond to other models when a phase transition (10.1002/mma.6965, 2020) occurs. Also, we obtain the critical point using a new analytical method.

KEYWORDS:

Thermodynamics, Random connection model, Stochastic geometry, Phase transition, Statistical mechanics

1 | INTRODUCTION

The discussion of mathematical and stochastic models of infectious diseases, which are widely used in epidemiology, is of interest to every human community. These models provide an understanding of the underlying mechanisms by which epidemic outbreaks in a given population are addressed. In this way, decisions can be made to control or prevent the epidemic [1,2]. One of the most widely used mathematical models to describe this type of problem is a random connection model (RCM) [3]. The RCM of continuum percolation is a generalization of random geometric graph with two sources of randomness, the point locations and their links [4,5]. The probability of existence of an edge between two points decreases as the distance between two points increases. It seems that the RCM was studied for the first time by Gilbert [6] as a model of communication networks. Gilbert's model is the special case of the RCM when the probability of connection is of the Boolean, zero-one type. This geometrically corresponds to placing discs of radius $r > 0$ at points and considering connected components formed by clusters of overlapping discs [7]. Such a model is the simplest Boolean model of continuum percolation in percolation theory and stochastic geometry. The most basic objects studied in stochastic geometry are point processes, where a point process can be represented as a random collection of points in space. For example, the location of the nodes in the communication networks can be modeled as random, such as a Poisson point process. Also in the RCM, points are placed in space based on the Poisson point process. For any two points x and y of the Poisson point process, an edge is added between them with the connection function $g(|x - y|)$, independently of

all other pairs of points of the Poisson point process where |.| denotes the usual Euclidean distance[8]. These edge connections lead to the formation of clusters of points, also known as a soft random geometric graph[9]. This model is quite general and has applications in different branches of science. As mentioned, in epidemiology the probability that an infected herd at location x infects another herd at location y[10,11]; in telecommunications the probability that two transmitters are non-shaded and can exchange messages[12]; in biology the probability that two cells can sense each other. Also, this and related models have been studied in the contexts of geometric probability, statistics and physics[13,14,15,16]. In physics, continuum percolation is applied to study the clustering behavior of particles in continuum systems and is relevant to phenomena like conduction in dispersion, flow in porous media, elastic behavior of composites, solgel transition in polymers, aggregation in colloids, and the structure of liquid water, to name a few, see the works[17,18,19,20] and references therein.

Although Gilbert's focus was the study of communications networks, he noted that a resulting infinite graph could also model the spread of a contagious disease. Gilbert discussed percolation theory by defining a critical value when an infinitely connected cluster is formed. In other words, for values larger than the critical value, there is a non-zero probability that the disease spreads, or that communication is possible to some arbitrarily distant nodes of the network. So, we say that the model has percolated that is a phase transition has occurred. According to a connectivity and percolation theory are the most important focus of much research, this paper studies such certain properties of the RCM. In particular, for the RCM with the connection function $g(x) = I_{\{|x|\leq 1\}}$, we study the thermodynamic properties and probability distribution moments of this model at the point where the percolation occurs. First, we consider concepts such as free energy, internal energy and entropy in the statistical mechanics of extensive and non-extensive[21,22,23]. Given the relationship between these quantities, we obtain three probability functions in which the process is similar to the probability function presented by Penrose[24]. Also, a detailed description of the relationship between these three probability functions provides a suitable approximation for the probability function presented by Penrose. Finally, we discuss the concept of phase transition and percolation by examining some thermodynamic quantities[25] and the moments of the probability distribution, including free energy, magnetization, kurtosis, mean and variance. We observed the fluctuations of the most of the quantities studied for the RCM with the connection function $g(x) = I_{\{|x|\leq 1\}}$ or the Poisson plob model in terms of temperature parameter are similar to the fluctuations in the two-dimensional Ising model[26,27]. These fluctuations play a central role in our understanding of phase transition. Their behavior near a critical point provides important information about the underlying many-particle interactions. Perhaps one of the systems studied in statistical physics that can show phase transition is the Ising model[28]. This model can also be used in the area of epidemiology to study the properties that are responsible for the spread of diseases.

There is substantial interest in these types of results in one class of applications in wireless communications[29,30]. In our setting, the connected components are of interest because they represent long-range or short-range communication. Our technique introduces functions that calculate the probability of placing an arbitrary point inside a connected component consisting of k points, whereby the system is able to communicate, under the condition that k tends to infinity. It is worth noting that this is the favorite discussion in percolation theory, i.e., the existence of unbounded connected components. These reasons give us a motivation to organize this paper as follows. In Section 2, we describe the RCM and define the thermodynamic quantities used throughout this paper. The results are discussed in Section 3. In Subsection 3.1, using a comparison of three functions of free energy, internal energy and entropy, three probability functions are calculated and their relationship to each other is expressed in detail. Finally in Subsection 3.2, we propose a mathematical method using the ratio of two consecutive probability values to determine the critical point and the occurrence of the percolation. Also, some thermodynamic quantities are plotted to determine the phase transition in this model.

2 | THE INTRODUCTION TO A CONTINUUM PERCOLATION MODEL

We consider the RCM of continuum percolation where the points x and y of a homogeneous Poisson point process are connected with probability $g(|x-y|)$ for a given g. The RCM in Euclidean space R^d with connection function g can be described as follows: let $\eta' = \{x_1, x_2, \dots\}$ be a homogeneous Poisson point process with parameter ρ on R^d and $g : R^d \to [0,1]$ be a measurable and symmetric function and that $0 < \int_{R^d} g(x)dx < \infty$. The number ρ is the characteristic parameter of the homogeneous Poisson point process, which represents the mean number of points in a set of unit volumes. It is called the intensity or density of the homogeneous Poisson point process[31]. Fix $x_0 = 0$, the origin, and let $\eta = \{x_0, x_1, \dots\}$. Given two points x_i and x_j of η (with $i > j$), connect them by an edge with probability $g(|x_i - x_j|)$ independently of all other pairs of points and the process η. This yields the RCM, an undirected random graph $G(\eta)$ with vertex set η. A component (cluster) of this graph is a maximally

connected subset of η. The cluster at the origin, $C(0)$, is the vertex set of the connected component of G which contains the origin[7,14]. Denote by $n[C(0)]$ the number of points (including 0) in $C(0)$, so that $n[C(0)]$ is a random variable taking values in $\{1, 2, \dots\}$. Let $q_k(\rho)$ denote the probability that $C(0)$ consists of k points, when η has intensity ρ. That is,

$$q_k(\rho) = p(n[C(0)] = k); \qquad k = 1, 2, \dots$$

For any measurable and bounded set Υ on R^d and $k \in \{1, 2, \dots\}$, Penrose[32] proved, in any dimension,

$$\begin{aligned} q_k(\rho) &= p_\rho(n[C(0)] = k, C(0) \subset \Upsilon) \\ &= \rho^{(k-1)}/(k-1)! \int_\Upsilon \cdots \int_\Upsilon g_2\left(0, x_1, \dots, x_{k-1}\right) \\ &\times \exp\{-\rho \int_\Upsilon g_1\left(y; \{0, x_1, \dots, x_{k-1}\}\right) dy\} dx_1 \dots dx_{k-1}, \end{aligned} \tag{1}$$

where g_1 denoted the probability that x_0 is not isolated in the random graph G[9] and defined by

$$g_1(x_0; c) = 1 - \prod_{j=1}^{k} \left(1 - g(x_0 - x_j)\right) \tag{2}$$

and, $g_2(x_0, x_1, \dots, x_k)$, the probability that this random graph is connected, is[33]

$$g_2(x_0, x_1, \dots, x_k) = \sum_{G \in G^c_{k+1}} \prod_{(i,j) \in G} g_{ij} \prod_{(i,j) \in G} (1 - g_{ij}),$$

where the summation is over all connected graphs G^c_{k+1} on points of c and largest cluster of size $(k+1)$.

Penrose[32] rigorously derived this integral for $p_k(\rho)$ in any dimension d, which this probability can be computed rather handily in one dimension. But this integral can not be calculated analytically and hence require approximate evaluation in the higher dimension. Penrose[24] then provided an approximation of this probability function in a particular case. He considered the homogeneous Poisson process of rate $\rho = y/c_d$ on R^d for $y > 0$, where $c_d = \pi^{(d/2)}/\Gamma((d/2)+1)$ is the volume of the ball of unit radius in dimension d. In this paper, it is proved that for $r = 1$ and $p = 1$, as $d \to \infty$ with constant y, the following limit relation is established.

$$q_k(\rho) \to p_k(y) = \frac{k^{k-2}}{(k-1)!} y^{k-1} e^{-ky}; \qquad k = 1, 2, \dots. \tag{3}$$

As mentioned, $q_k(\rho)$ is the cluster distribution. By analogy with the Ising model, we introduce the magnetization function as[34,35]

$$M(\rho, h) = 1 - \sum_{k=0}^{\infty} q_k(\rho) e^{-kh}; \qquad h \geq 0, \tag{4}$$

where h is the external magnetic field. By setting $h = 0$ in the magnetization function,

$$M(\rho, 0) = p(n[C(0)] = \infty).$$

Using the term by term differentiation, we have

$$\lim_{h \to 0^+} \frac{\partial M(\rho, h)}{\partial h} = \mathbb{E}_\rho[n[C(0)] I_{\{n[c(0)] < \infty\}}] = \chi^{(1)}(\rho).$$

$\chi^{(1)}(\rho)$, which is obtained by differentiating the magnetic field M with respect to h, is called the mean cluster size. It is the analogue of the (isothermal) susceptibility of magnetic systems. Also, the following limit relationship is established for any $N \in R$.

$$(-1)^{(N+1)} \lim_{h\to 0^+} \frac{\partial^N M(\rho,h)}{\partial h^N} = \mathbb{E}_\rho[n[C(0)]^N I_{\{n[c(0)]<\infty\}}] = \chi^{(N)}(\rho). \tag{5}$$

More precisely, $\chi^{(N)}(\rho)$ is the N^{th} moment of the size of the cluster at an arbitrary point of Γ, discounting infinite clusters. The free energy $F(\rho,h)$ is defined by[35,36]

$$F(\rho,h) = h(1-q_0(\rho)) + \sum_{k=1}^{\infty} \frac{1}{k} q_k(\rho) e^{-kh}; \qquad h \geq 0. \tag{6}$$

The second term in the above phrase was first presented by Kasteleyn and Fortuin to regulate a correspondence between values for percolation and similar values for magnetic systems. If we differentiate the free energy $F(\rho,h)$ with respect to h, we get

$$\frac{\partial F(\rho,h)}{\partial h} = M(\rho,h).$$

The zero-field free energy $F(\rho,0)$ is a more interesting subject of study. By our definition,

$$\begin{aligned} F(\rho,0) = \mathbb{E}_\rho[n[C(0)]^{-1} I_{\{n[c(0)]<\infty\}}] &= \sum_{k=1}^{\infty} \frac{1}{k} q_k(\rho) \\ &= \chi^{(-1)}(\rho). \end{aligned} \tag{7}$$

Grimmett[37] discovered that the zero-field free energy or the cluster density coincides with the number of clusters per vertex. Penrose proved the continuity of the cluster density in ρ for the case $g(x) = I_{\{|x|\leq r\}}$ [32]. Also, he provided upper and lower bounds the zero-field free energy for this connection function.

3 | RESULTS

As mentioned, the RCM has applications in many sciences that can also be seen as a model for an epidemic spread. Therefore, the following is investigating the thermodynamic quantities and the phase transition in the critical point of this model and its similar performance to other mathematical models including the Ising model[38]. In this research, case studies run in R-3.1.2.

3.1 | The relationship between free energy, entropy and internal energy

This subsection is devoted to introduce the thermodynamic relations between free energy, entropy and internal energy. We consider the Helmholtz free energy[39] as

$$F = U - \beta S, \tag{8}$$

where U and S are the internal energy and entropy, respectively. Also, β is a positive constant and can be eliminated by the proper unit. We consider different definitions of these three quantities, i.e., U, S and F in the literature of statistical mechanics of extensive and non-extensive[40].

In the first case, we consider

$$U = \sum_{k=1}^{\infty} k\ p_k(\rho).$$

The BG-shannon entropy is

$$S = -\sum_{k=1}^{\infty} p_k(\rho)\ \ln p_k(\rho). \tag{9}$$

We replace the zero-field free energy $F(\rho,0)$ given in Equation 7 instead of the Helmholtz free energy, F. Thus, Equation 8 can be written in the following form:

$$\sum_{k=1}^{\infty} \frac{1}{k} p_k(\rho) = \sum_{k=1}^{\infty} k p_k(\rho) + \beta \sum_{k=1}^{\infty} p_k(\rho) \ln p_k(\rho).$$

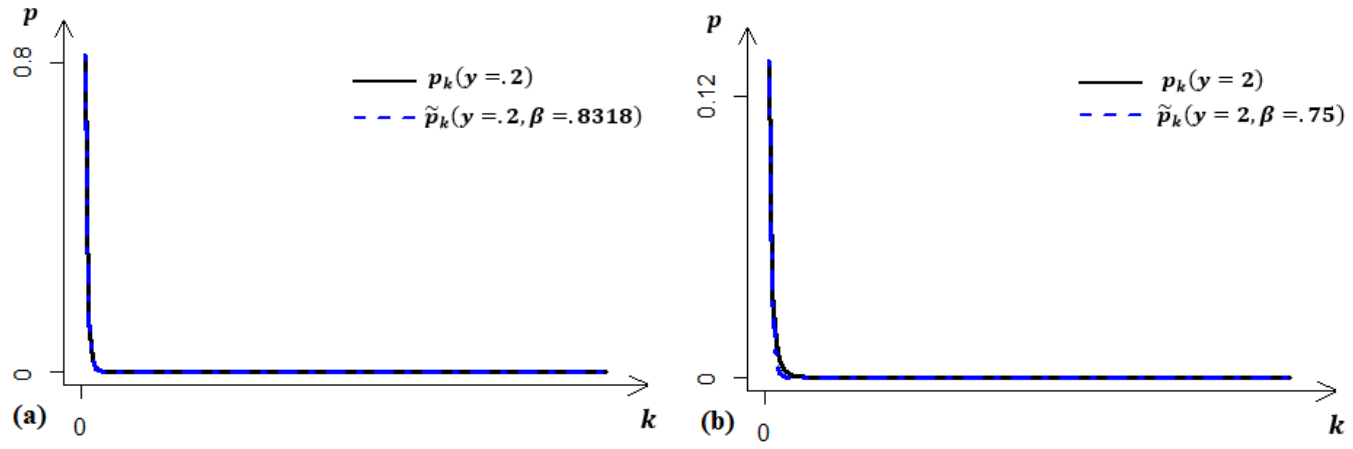

FIGURE 1 The illustration of the functions of $p_k(y)$ and $\tilde{p}_k(y, \beta)$.

Putting relationships on one side gives us

$$\sum_{k=1}^{\infty} \Big(\frac{1}{k} - k - \beta \ln p_k(\rho) \Big) p_k(\rho) = 0.$$

Then, under the constraint $\sum_{k=1}^{\infty} p_k = 1$, p_k is obtained as follows

$$p_k = e^{\frac{1}{\beta}(\frac{1}{k} - k)} / \sum_{k=1}^{\infty} e^{\frac{1}{\beta}(\frac{1}{k} - k)}. \tag{10}$$

The changes of the function p_k in terms of k with the parameter β are shown in Figures 1 and 2 . The interesting point about the function p_k is the existence of the relationship between this function with the approximation function provided by Penrose in Equation 3. By calculating and evaluating the function p_k in Equation 10, we arrive at the following function, which is very close to the function presented by Penrose.

$$\tilde{p}_k(y, \beta) = \begin{cases} e^{\frac{1}{\beta}(\frac{1}{k} - k)} / \sum_{k=1}^{\infty} e^{\frac{1}{\beta}(\frac{1}{k} - k)} & y < 1 \\ e^{\frac{1}{\beta}\left(\frac{1}{k+1} - (k+1)\right)} & y \geq 1 \end{cases} \tag{11}$$

In Equation 11, for values less than the critical value of the intensity parameter, i.e., $y_c = 1$, we can find $\beta < 2.685$ such that the standard function p_k is the good approximation for the function $p_k(y)$. On the other hand, the non-standard function p_k, for values greater than this critical value and by removing the first value with very little error, has the same function as the approximation function provided by Penrose. These behaviors are clearly shown in Figure 1 . In this figure, the functions $\tilde{p}_k(y, \beta)$ and $p_k(y)$ are shown with the dashed line and continuous line, respectively. In two cases $y = .2, \beta = .8318$ and $y = 2, \beta = .75$, the relationship between these functions is shown in the parts (a) and (b) of this figure. As can be seen in Figure 1 , two functions $\tilde{p}_k(y, \beta)$ and $p_k(y)$ clearly overlap.

In order to obtain the error rate for this approximation technique, which is actually the difference between the estimated values and what is estimated, we calculate the mean squares of the error, i.e., $MSE = \sum_{i=1}^{k} (p_i(y) - \tilde{p}_i(y, \beta))^2 / k$. The mean squares of the error of these two functions are calculated for some values of y and β in Tables 1 and 2 . According to Table 1 , as the intensity parameter becomes smaller, the value of the estimation error also becomes smaller so that it eventually tends to zero. Also in this table, when the value of β decreases, parameter y also decreases in the same direction. But in Table 2 , the value β that results in the least error, decreases as the intensity parameter increases. That is, for $y \to \infty$ and $\beta \to 0$, the mean squared error tends to zero at infinity.

In the second case, we want to know how the form of the function $p_k(\rho)$ changes if we use the functions given in Equations 13 and 12 instead of BG-Shannon entropy and internal energy. Tsallis entropy and q-internal energy or unnormalized q-expectation

TABLE 1 The MSE for $y < 1$.

y	β	**MSE**
0.9	2.3948	6.7e-05
0.5	1.4334	8.1e-06
0.4	1.22862	2.9e-06
0.3	1.03066	5.9e-07
0.2	0.8318	1.3e-08
0.05	0.48878	1.3e-08

TABLE 2 The MSE for $y \geq 1$.

y	β	**MSE**
1	1.5	2.3e-05
2	0.75	1.3e-06
3	0.5	5.8e-08
4	0.375	2.1e-09
5	0.3	5.7e-11
20	0.075	5.5e-34

value are defined[41], respectively as

$$S_q = \frac{1}{q-1}\Big(\sum_{k=1}^{\infty} p_k(\rho)^q - 1\Big), \tag{12}$$

and

$$U_q = \sum_{k=1}^{\infty} k p_k(\rho)^q. \tag{13}$$

U_1 corresponds to the standard mean value of the quantity k. The value q is an adjustable parameter of non-extensivity namely entropic index. Tsallis entropy is defined as the measurement of uncertainty and disorder about obtained information in a system[42]. In other words, the defined entropy is main core of non-extensive statistical mechanics. Tsallis entropy also illustrates long-memory and long-range interaction of the systems. By setting $\beta = 1$ in Equation 8, we have

$$\sum_{k=1}^{\infty} \frac{1}{k} p_k(\rho) = \sum_{k=1}^{\infty} k p_k(\rho)^q - \frac{1}{q-1}\Big(\sum_{k=1}^{\infty} p_k^q - 1\Big),$$

or,

$$\sum_{k=1}^{\infty} p_k(\rho)\Big[\Big(\frac{(q-1)}{k} - (q-1)k p_k(\rho)^{(q-1)} + p_k(\rho)^{(q-1)}\Big)\Big] - 1 = 0.$$

To find an approximation formula, using the normalized condition $\sum_{k=1}^{\infty} p_k = 1$ and the fact that $p_k(\rho) \geq 0$, we get

$$p_{q,k}^{(1)} = \Big[\frac{1 - \frac{(q-1)}{k}}{1-(q-1)k}\Big]^{\frac{1}{(q-1)}} \Big/ \sum_{k=1}^{\infty}\Big[\frac{1 - \frac{(q-1)}{k}}{1-(q-1)k}\Big]^{\frac{1}{(q-1)}}. \tag{14}$$

Here, the index q takes values less than 1 because $p_{q,k}^{(1)} \geq 0$. This function is plotted in Figure 2 for the different values of q, which is shown in the parts (a), (b), (e) and (f) of this figure. According to these parts, when the value of q decreases, the range of values adopted by the function $p_{q,k}^{(1)}$ clearly increases. Now, we compare this function with the function p_k in Equation 10. These functions are plotted in parts (a) and (b) of Figure 2 for some of the values q and β. The mean squared error of these functions in part (a) with parameters $q = -.1$ and $\beta = 5.4$ is equal to $9.9e-05$. In the case of $q \to -\infty$ and $\beta = 1.36$, the mean

squared error of these functions is $3.1e-05$ which its diagram is seen in part (b) of Figure 2 . As can be seen in this figure, when β tends to 1 and q to $-\infty$, the overlap of these functions relative to each other clearly increases.

In the third case, we consider Tsallis entropy in Equation 12, the q-internal energy in Equation 13 and the unnormalized q-zero-field free energy as follows

$$F = \sum_{k=1}^{\infty} \frac{1}{k} p_k(\rho)^q. \tag{15}$$

By setting $\beta = 1$ in Equation 8,

$$\sum_{k=1}^{\infty} \frac{1}{k} p_k(\rho)^q = \sum_{k=1}^{\infty} k p_k(\rho)^q - \frac{1}{q-1}(\sum_{k=1}^{\infty} p_k^q - 1),$$

and putting relationships on one side of equality,

$$\sum_{k=1}^{\infty} p_k^q \Big[\frac{(q-1)}{k} - (q-1)k + 1\Big] - 1 = 0.$$

Using the condition of $\sum_{k=1}^{\infty} p_k = 1$, we can write

$$p_{q,k}^{(2)} = \Big[\frac{1}{\frac{(q-1)}{k} - (q-1)k + 1}\Big]^{\frac{1}{(q-1)}} / \sum_{k=1}^{\infty} \Big[\frac{1}{\frac{(q-1)}{k} - (q-1)k + 1}\Big]^{\frac{1}{(q-1)}}. \tag{16}$$

Since $p_{q,k}^{(2)} \geq 0$, the entropic index q can take values less than 1. The function $p_{q,k}^{(2)}$ is shown in the parts (c), (d), (e) and (f) of Figure 2 for the different values of q. According to this figure, by decreasing the value of q, the range of values accepted by the function $p_{q,k}^{(2)} \geq 0$ clearly increases so that it takes almost only two values of 1 and 0. In the following, we will deal with the relationship between the function $p_{q,k}^{(2)}$ and the functions p_k and $p_{q,k}^{(1)}$. The diagram of the functions $p_{q,k}^{(2)}$ and p_k is plotted in parts (c) and (d) of Figure 2 . The mean squared error of these functions is obtained 0.0001 for $q = -11$ and $\beta = 1$. These functions overlap well when q tends to $-\infty$ and β to 0. That is, their mean squared error is very close to zero, which is clearly seen in part (d) of Figure 2 . In fact, for these two functions, the following limit relation can be written.

$$\lim_{\beta \to 0} p_k = \lim_{q \to -\infty} p_{q,k}^{(2)}, \qquad \forall k \in R. \tag{17}$$

Finally, we compare the functions of $p_{q,k}^{(1)}$ in Equation 14 and $p_{q,k}^{(2)}$ in Equation 16. The diagram of these functions is drawn in parts (e) and (f) of Figure 2 . The mean squared error of these functions in part (e) of this figure is $8.8e-05$. Whereas, as shown in part (f) of this figure, when the parameter q tends to 1, the value of this error is zero. Hence, we have

$$\lim_{q \to 1^-} p_{q,k}^{(1)} = \lim_{q \to 1^-} p_{q,k}^{(2)}, \qquad \forall k \in R. \tag{18}$$

3.2 | The fluctuations of the random connection model

Now, we want to discuss a very interesting concept called percolation[43]. In the RCM, the percolation probability, i.e., the probability that there exists an infinite cluster is

$$\psi(\rho) = P(n[C(0)] = \infty),$$

and the critical intensity defined as

$$\rho_c = \sup\{\rho : \psi(\rho) = 0\}.$$

Based on the fundamental theorem presented by Penrose, $y_c (= \rho c_d) \in (0, \infty)$ and $\lim_{d \to \infty} y_c = 1$ are shown[24]. Here, we want to present mathematical and physical analytical methods to find this critical point. Thus, we first obtain this critical point using the mathematical analytical method. For this purpose, the ratio of two consecutive probabilities $p_k(y)$ and $p_{k+1}(y)$ is

$$\frac{p_{k+1}(y)}{p_k(y)} = y e^{-y} (1 + \frac{1}{k})^{k-1}. \tag{19}$$

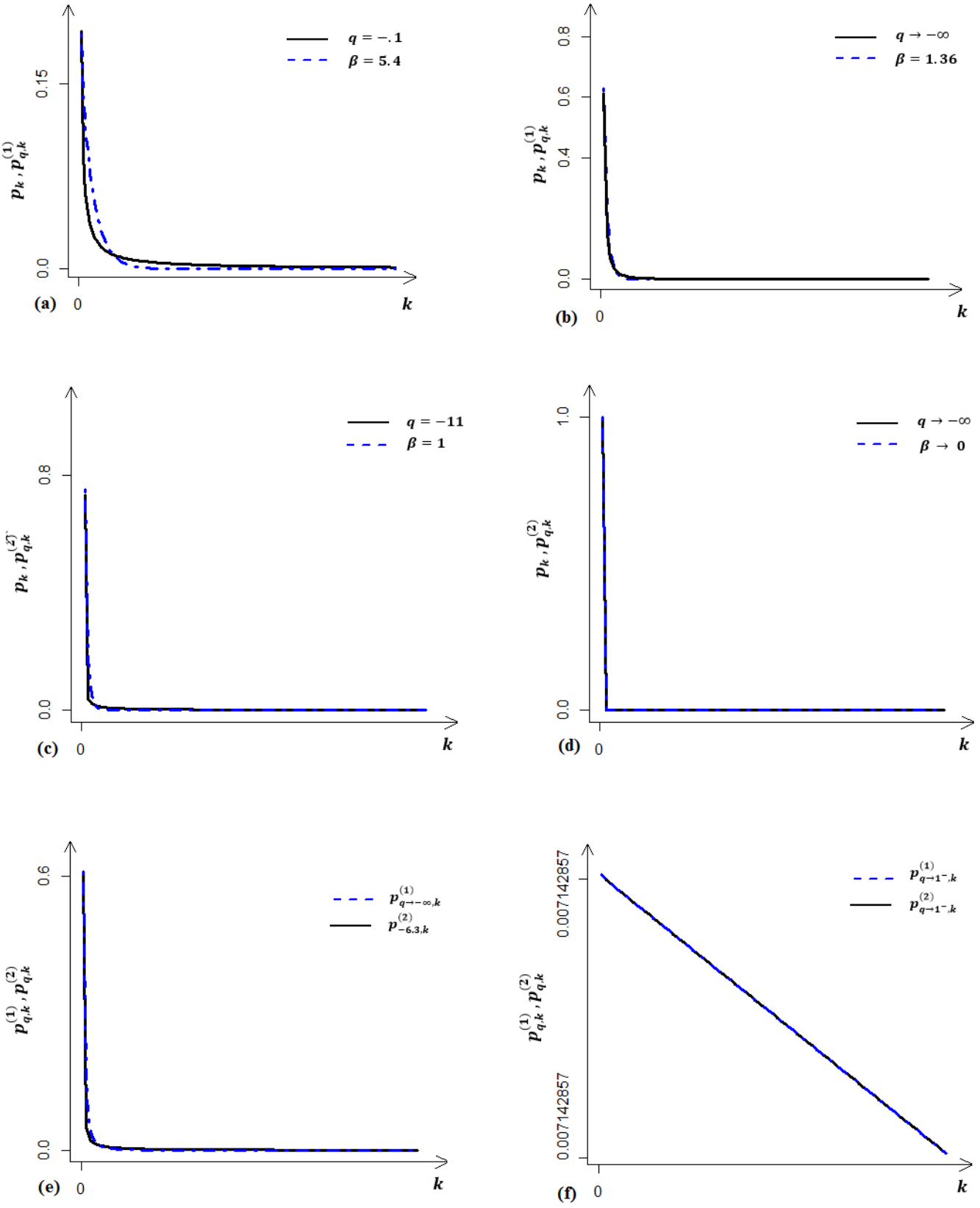

FIGURE 2 The illustration of relationship between the functions of p_k, $p_{q,k}^{(1)}$ and $p_{q,k}^{(2)}$.

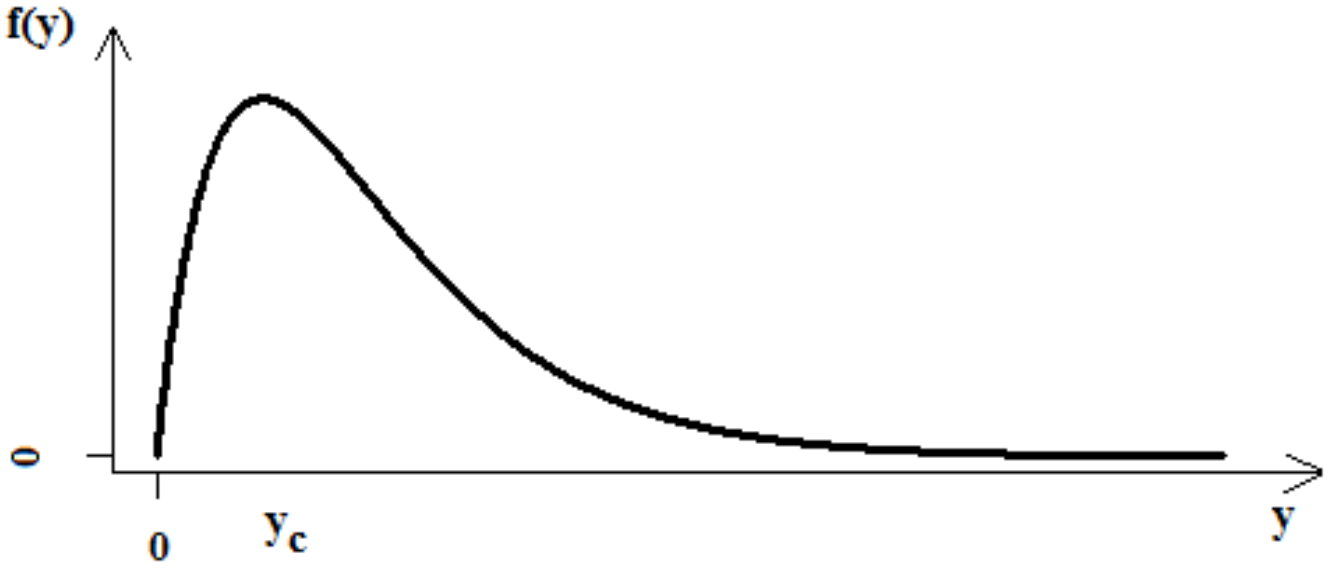

FIGURE 3 The limit of the ratio of two consecutive probabilities $p_k(y)$ and $p_{k+1}(y)$ with respect to y.

The diagram of the function $f(y) = \lim_{k\to\infty} p_{k+1}(y)/p_k(y)$ is drawn in Figure 3 . As can be seen, the slope of the function varies around a maximum point. In fact, this maximum point is exactly the same as the critical point $y_c = 1$. We expect that at this value the model exhibit some kind of critical behavior, but we will not present its more detailed analysis here.

On the other hand, in the physics' literature, the matter has different states. For instance, gas, liquid, solid, magnetic ordering, superconducting and superfluid states can exist in different materials. When the matter transits from one state to another state, the phase transition occurs in the system. In standard statistical physics, the histogram of thermodynamic quantities is often used to detect the nature of the phase transition and the percolation point. Among these quantities that can be examined are the magnetization function, the cluster mean, variance, free energy and the kurtosis. The first interesting quantity we consider is the magnetization function $M(y, h)$ in Equation 4 for the approximation function provided by Penrose in the Poisson blob model. The magnetization versus the intensity parameter, ρ, is shown in part (a) of Figure 4 . The magnetization is zero for values less than the critical value $y_c = 1$, and as the intensity parameter increases, the model magnetization reaches its highest level of 1 which is shown in this figure. Moreover, as the size of the cluster increases, the magnetization near the critical parameter suddenly increases. The interesting point about this model is that it shows well the behavior similar to the phase change of magnetic systems from the paramagnetic phase to the ferromagnetic phase. In fact, these magnetization changes in terms of the intensity parameter in the Poisson blob model are exactly the same as temperature changes of magnetization in the Ising model. Also, Figure 4 shows the changes of spontaneous magnetization against temperature for the two-dimensional Ising model of different sizes[24]. Of course, as mentioned, the zero of the magnetization function is equivalent to the fact that for $y < y_c$ there is no possibility of percolation, and this means that an infinite cluster is not formed[24]. In part (b) of Figure 4 , the zero-field free energy versus intensity parameter is plotted for the Poisson blob model of different sizes. It is observed that the zero-field free energy for values greater than the intensity parameter approaches zero while at the critical point it is 1/2.

Figure 5 shows the mean and variance of the cluster size versus intensity parameter for different sizes. As shown in this figure, peaks in both of these quantities appear in the critical parameter. Also, the peak of these quantities decreases with decreasing cluster size and gets closer to the intensity parameter axis on the coordinate axis. As shown in Figure 5 , the trend of changes in the mean and variance quantities is almost the same. According to these explanations, it can be concluded that the intensity parameter changes, y, are similar to the temperature changes, T, in classical systems. More specifically, we observed that the mean and variance of the cluster size versus the intensity parameter are equivalent to specific heat and magnetic sensitivity versus temperature in the 2D classical Ising model with different sizes[44].

Finally, we plot entropy in Equation 9 and a quantity called kurtosis versus intensity parameter for the Poisson blob model of different sizes in Figure 6 . The kurtosis is defined in statistical physics by $B = \frac{<s_4>}{<s_2>^2}$, where $< s_2 >$ and $< s_4 >$ denote the second and fourth moments of the cluster size. Due to the sensitivity of kurtosis and entropy quantities, these quantities change significantly when the intensity parameter and the cluster size change. Therefore, the kurtosis and entropy can be used

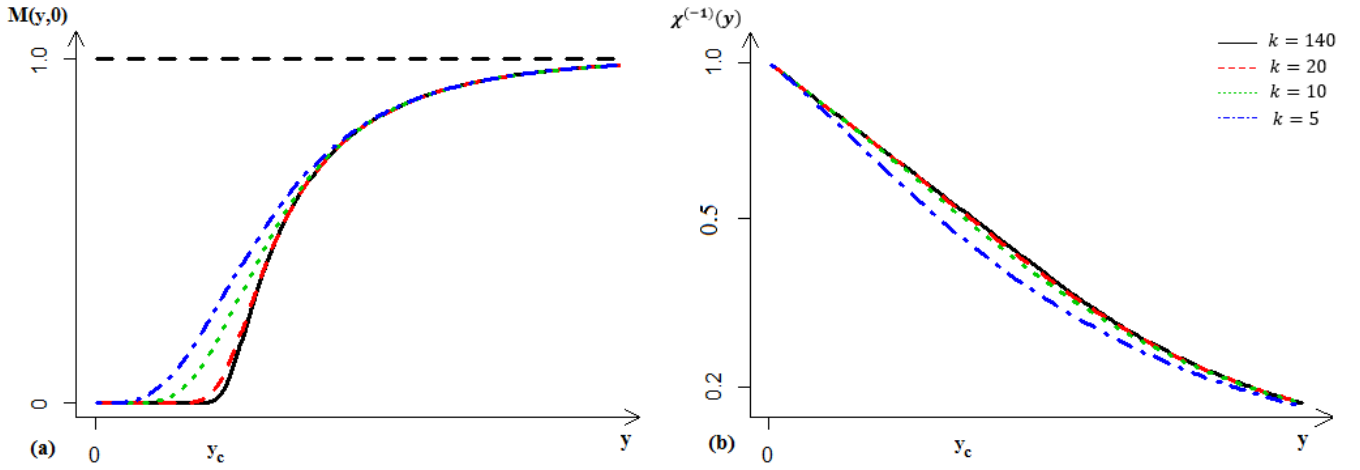

FIGURE 4 The magnetization (*a*) and zero-field free energy (*b*) versus the intensity parameter in Poisson blob model with different sizes.

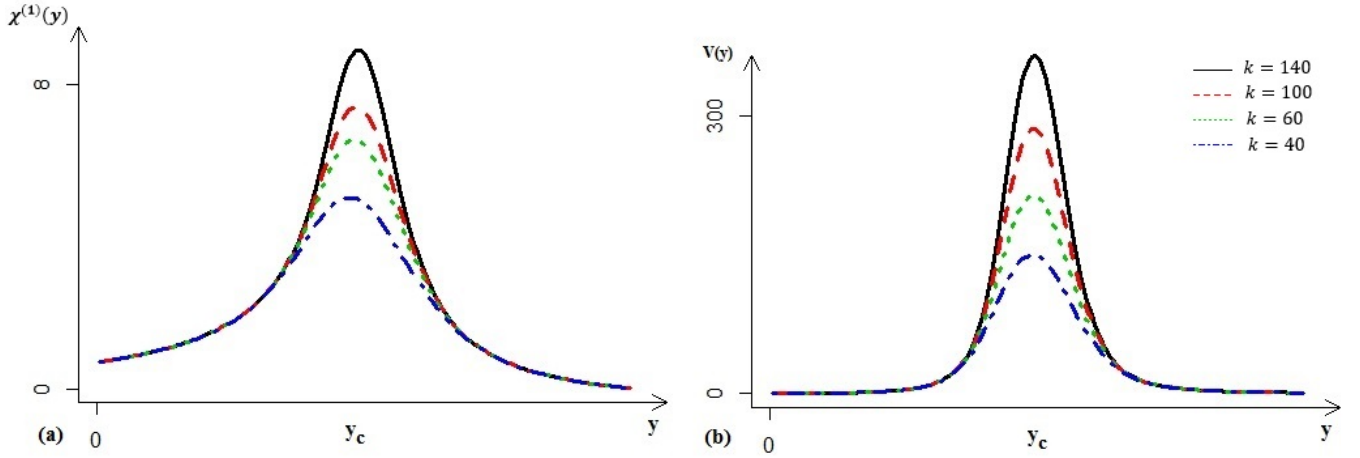

FIGURE 5 The mean (*a*) and variance (*b*) of the cluster size versus the intensity parameter in Poisson blob model with different sizes.

to accurately determine the critical intensity value. It also seems that the kurtosis coefficient has a similar role to the Binder ratio in statistical physics to accurately determine the phase transition points in the numerical simulation of different models[45]. Here, the minimum value of the kurtosis coefficient occurs at the critical point.

4 | CONCLUSIONS

We study the connected components of RCM on the Poisson point process, which is obtained by connecting points with probabilities that depend on their relative position. In this paper, we use the relationships between free energy, internal energy, and entropy to obtain the probability functions that are closely related to the probability function provided by Penrose. The relationship between these calculated probability functions is shown precisely in the figure (2). Moreover, in the second part of the results, we present mathematical and physical analytical methods to show the phase transition at the critical point. That is, by providing a limit function, the critical point occurs exactly at the root of the first-order derivative. Finally, using the approximation function provided by Penrose in the Poisson blob model, we calculated and investigated the statistical and thermodynamic quantities such as the magnetization function, zero-field free energy and etc.

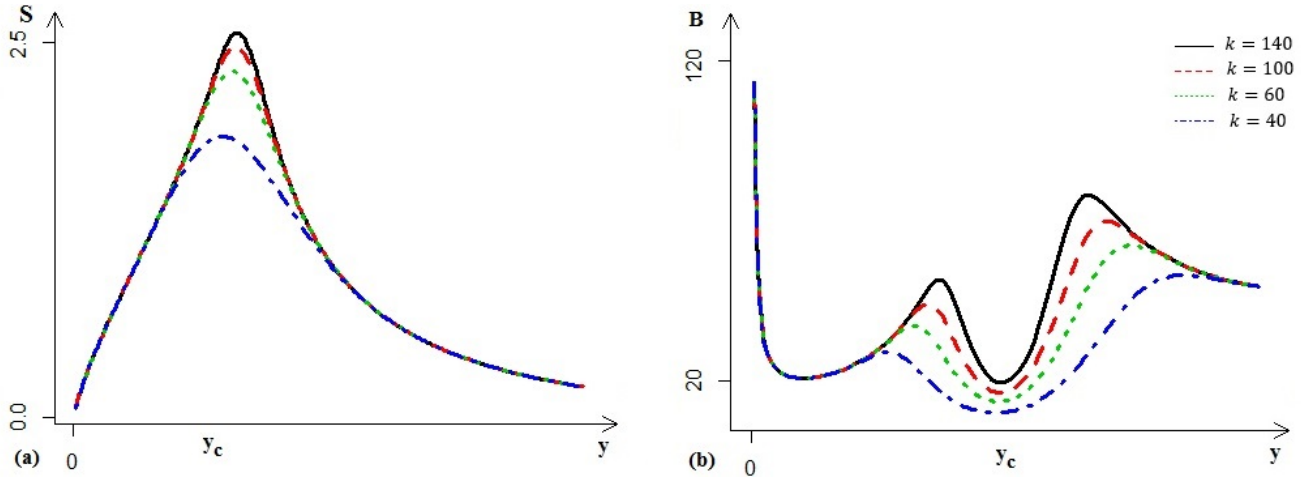

FIGURE 6 The entropy and kurtosis versus the intensity parameter in Poisson blob model with different sizes.

References

1. Rothman K, Greenland S, Lash T. *Modern Epidemiology (3rd Ed)*. Philadelphia: Lippincot Williams & Wilkins; 2012. ISBN 978-1-4511-9005-2.
2. Eubank S, Guclu H, Kumar VSA, et al. Modelling disease outbreaks in realistic urban social networks. *Nature.* 2004;429(6988):180–184.
3. Roy R, Sarkar A. High density asymptotics of the poisson random connection model. *Phys A.* 2003;318(1-2):230–242.
4. Penrose MD. *Random Geometric Graphs*. Oxford: Oxford University Press; 2003. ISBN 978-0198506263.
5. Müller T, Prałat P. The acquaintance time of (percolated) random geometric graphs. *Eur J Comb.* 2015;48:198–214.
6. Gilbert EN. Random plane networks. *J Soc Indust Appl Math.* 1961;9(4):533–543.
7. Grimmett GR. *Percolation*. Berlin: Springer−Verlag; 1999. ISBN 3-540-64902-6.
8. Dettmann CP, Georgiou O. Random geometric graphs with general connection functions. *Phys Rev E.* 2016;93(3):032313.
9. Penrose MD. Connectivity of soft random geometric graphs. *Ann Appl Probab.* 2016;26(2):986–1028.
10. May R.M, Anderson RM. *Infectious Diseases of Humans*. Oxford: Oxford University Press; 1991. ISBN 0-19-854599-1.
11. Cristina GAL, Eduardo M, Luis FL, Marcos A. Analogy between the formulation of Ising-Glauber model and Si epidemiological mode. *Appli Math and Phy.* 2019;7(5):1052–1066.
12. Franceschetti M, Meester R. *Random Networks for Communication*. Cambridge: Cambridge University Press; 2007. ISBN 978-0521854429.
13. Amin M. Energy: The smart grid solution. *Nature.* 2013;499(7457):145–147.
14. Meester R, Roy R. *Continuum Percolationn*. Cambridge: Cambridge University Press; 1996. ISBN 978-0511895357.
15. Penrose MD. Single linkage clustering and continuum percolation. *J Multivariat Anal.* 1995;52(1):94–109.
16. Hall PG. *Introduction to Coverage Processes*. New York: Wiley; 1988. ISBN 978-0471857020.
17. Quintanilla J, Torquato S, Ziff RM. Efficient measurement of the percolation threshold for fully penetrable discs. *J Phys A:Math Gen.* 2000;33(42):399–407.

18. Quintanilla J, Torquato S. Clustering in a continuum percolation model. *Adv Appl Probab.* 1997;29:327–336.

19. Sadeghnejad S, Masihi M. Point to point continuum percolation in two dimensions. *J Stat Mech.* 2016;10:103210.

20. Klatt MA, Schröder −Turk GE, Mecke K. Anisotropy in finite continuum percolation: threshold estimation by Minkowski functionals. *J Stat Mech.* 2017;2:1–28.

21. Gokhan BB. The Physical meaning of the Renyi relative entropy. *J Nat Appl Sci.* 2017;21(1):292–295.

22. Hao G, Hong Q. The Physical origins of entropy production, free energy dissipation and their mathematical representations. *Phys Rev E.* 2010;81:051133.

23. Liangrong P, Hong Q, Liu L. Thermodynamics of markov processes with non-extensive entropy and free energy. *Phys Rev E.* 2020;101:022114.

24. Penrose MD. Continuum percolation and euclidean minimal spanning trees in high dimensions. *Ann Appl Probab.* 1996;6(2):528–544.

25. Gupta MC. *Statistical Thermodynamics*. New Delhi, India: New Age International; 2007. ISBN 978-8122410662.

26. Binder K. Finite size scaling analysis of Ising model block distribution functions. *Z Phys B.* 1981;43:119–140.

27. Davatolhagh S, Moshfeghian M, Saberi AA. Critical behavior of the geometrical spin clusters and interfaces in the two-dimensional thermalized bond Ising model. *J Stat Mech.* 2012;02:02015. https://doi.org/10.1088/1742-5468/2012/02/P02015.

28. Picco M, Sourlas N. On the phase transition of the 3D random field Ising model. *J Stat Mech.* 2014;03:03019. https://doi.org/10.1088/1742-5468/2014/03/P03019.

29. Giles AP, Georgiou O, Dettmann CP. Connectivity of Soft Random Geometric Graphs over Annuli. *J Stat Phys.* 2016;162:1068–1083.

30. Haenggi M, Andrews J, Baccelli F, Dousse O, Franceschetti M. Stochastic geometry and random graphs for the analysis and design of wireless networks. *IEEE J Sel Areas Commun.* 2009;27(7):1029–1046.

31. Chiur SN, Stoyan D, Kendall WS, Mecke J. *Stochastic Geometry and its Applications; 3nd ed*. Chichester: John Wiley & Sons; 2013. ISBN 978-0-470-66481-0l.

32. Penrose MD. On a continuum percolation model. *Adv Appl Probab.* 1991;23:536–556.

33. Dettmann CP, Georgiou O. Random geometric graphs with general connection functions. *Phys Rev E.* 2017;93:032313.

34. Zhang HI, Choi MY. Generalized formulation of free energy and application to photosynthesis. *Phys A.* 2018;493(3):125–134.

35. Zhang Y. A singularity at the criticality for the free energy in percolation. *arXiv: Probab.* 2020;. arXiv preprint math/0301160v6.

36. Zhang Y. A derivative formula for the free energy function. *J Stat Phys.* 2011;146(2):466–473.

37. Grimmett GR. On the differentiability of the number of clusters per vertex in percolation model. *J Lond Math Soc.* 1981;23(2):372–384.

38. Laudau DP, Binder K. *A Guide to Monte Carlo Simulations in Statistical Physics; 3nd ed*. Cambridge: Cambridge University Press; 2009. ISBN 978-0521768481.

39. Levine IN. *Physical Chemistry; 6nd ed*. Brooklyn, New York: Thomas Timp; 2009. ISBN 978-0-07-253862-5.

40. Singh N. On The Fundations of Statistical Mechanics: a Brief Review. *Mod Phys Lett B.* 2013;27(6):1330003.

41. Tsallis C. Non-extensive statistics: theoretical, experimental and computational evidences and connections. *Braz J Phys.* 1999;29(1):1–35.

42. Mehri A, Agahi H, Mehri Dehnavi H. A novel word ranking method based on distorted entropy. *Phys A.* 2019;521:484–492.

43. Durrett R, Nguyen B. Thermodynamic inequalities for percolation. *Commun Math Phys.* 1985;99:253–269.

44. Hui Min Z. Monte Carlo study on ferromagnetic phase transition of two-dimensional Ising model. In: Advances in Engineering Research, Joint International Information Technology, Mechanical and Electronic Engineering; October, 2016; Atlantis Press. https://doi.org/10.2991/jimec-16.2016.91.

45. Binder K, Heermann DW. *Monte Carlo Simulation in Statistical Physics: an Introduction*. New York: Springer; 2010. ISBN 978-3642031625.